Geochemistry Geophysics Geosystems G3

AN ELECTRONIC JOURNAL OF THE EARTH SCIENCES

Published by AGU and the Geochemical Society

Article

Volume 8, Number 8

28 August 2007

Q08013, doi:10.1029/2007GC001652

ISSN: 1525-2027

Hydrothermal activity on the ultra-slow spreading southern Knipovich Ridge

D. P. Connelly

National Oceanography Centre, Southampton SO14 3ZH, UK (dpc@noc.soton.ac.uk)

C. R. German

National Oceanography Centre, Southampton SO14 3ZH, UK

Woods Hole Oceanographic Institution, Woods Hole, Massachusetts 02543, USA

M. Asada and K. Okino

Ocean Research Institute, University of Tokyo, 1-15-1 Minamidai, Nakano, Tokyo 164-8639, Japan

A. Egorov

Shirshov Institute of Oceanology RAS, 36 Hakhimovsky, Moscow 117851, Russia

T. Naganuma

School of Biosphere Science, Hiroshima University, 1-4-4 Kagamiyama, Hikashi, Hiroshima 73908528, Japan

N. Pimenov

Institute of Microbiology, Russian Academy of Sciences, Prospect 60-Letija Oktyabrya 7/2, 117312 Moscow, Russia

G. Cherkashev

VNII Okeangeologia, 1 Anglyisky Avenue, St. Petersburg 190121, Russia

K. Tamaki

Ocean Research Institute, University of Tokyo, 1-15-1 Minamidai, Nakano, Tokyo 164-8639, Japan

[1] We report first evidence for hydrothermal activity from the southern Knipovich Ridge, an ultra-slow spreading ridge segment in the Norwegian-Greenland Sea. Evidence comes from optical backscatter anomalies collected during a systematic side-scan sonar survey of the ridge axis, augmented by the identification of biogeochemical tracers in the overlying water column that are diagnostic of hydrothermal plume discharge (Mn, CH_4, ATP). Analysis of coregistered geologic and oceanographic data reveals that the signals we have identified are consistent with a single high-temperature hydrothermal source, located distant from any of the axial volcanic centers that define second-order segmentation along this oblique ridge system. Rather, our data indicate a hydrothermal source associated with highly tectonized seafloor that may be indicative of serpentinizing ultramafic outcrops. Consistent with this hypothesis, the hydrothermal plume signals we have detected exhibit a high methane to manganese ratio of 2–3:1. This is higher than that typical of volcanically hosted vent sites and provides further evidence that the source of the plume signals reported here is most probably a high-temperature hydrothermal field that experiences some ultramafic influence (compare to Rainbow and Logachev sites, Mid-Atlantic Ridge). While such sites have previously been invoked to be common on the SW Indian Ridge, this may be the first such site to be located along the Arctic ultra-slow spreading ridge system.

Components: 6099 words, 5 figures, 1 table.

Keywords: hydrothermal; Arctic; serpentinization; Knipovich Ridge.

Index Terms: 1034 Geochemistry: Hydrothermal systems (0450, 3017, 3616, 4832, 8135, 8424); 3614 Mineralogy and Petrology: Mid-oceanic ridge processes (1032, 8416); 4825 Oceanography: Biological and Chemical: Geochemistry; 0718 Cryosphere: Tundra (9315).

Received 3 April 2007; **Revised** 25 June 2007; **Accepted** 3 July 2007; **Published** 28 August 2007.

Connelly, D. P., C. R. German, M. Asada, K. Okino, A. Egorov, T. Naganuma, N. Pimenov, G. Cherkashev, and K. Tamaki (2007), Hydrothermal activity on the ultra-slow spreading southern Knipovich Ridge, *Geochem. Geophys. Geosyst.*, *8*, Q08013, doi:10.1029/2007GC001652.

1. Introduction

[2] Thirty years after the first discovery of seafloor venting [*Corliss et al.*, 1979] the majority of the 50–60,000 km of global mid-ocean ridge crest remains completely unexamined for the presence of submarine hydrothermal activity [*Baker and German*, 2004]. Ultra-slow ridges have been notably overlooked; it was not until 1997 that the first evidence for hydrothermal activity on any ultra-slow ridge system was first reported, from the eastern SW Indian Ridge [*German et al.*, 1998]. Since then, further discoveries of hydrothermal plume signals have been reported from elsewhere on the SWIR [*Bach et al.*, 2002] and from the Gakkel Ridge, beneath Arctic ice cover [*Edmonds et al.*, 2003]. Subsequently, however, *Baker et al.* [2004] have noted that when normalizing hydrothermal incidence to basaltic magma supply rates, ultra-slow ridges appear to be considerably more efficient than other ridge systems in sustaining hydrothermal vent activity. Combined data from the Gakkel Ridge and SWIR indicate the presence of at least one hydrothermal field along every ~100 km of ultra-slow spreading ridge crest [*Baker and German*, 2004].

[3] In recent years the mid-ocean ridge system north of Iceland, including the Gakkel and Knipovich Ridges, has also been attracting interest from scientists interested in understanding the biogeography and biodiversity of deep-sea hydrothermal vent fauna [*Van Dover et al.*, 2002; *Tyler et al.*, 2002]. To date, more than 500 vent-endemic species, previously unknown to science, have been identified at hydrothermal fields in 6 distinct biogeographic provinces: SW Pacific, E Pacific, NE Pacific, Mid-Atlantic Ridge, Azores, Central Indian Ridge [*Van Dover et al.*, 2002]. The ridge crests north of Iceland are of particular interest because the land-bridge caused by the colocation of the Iceland hot spot and ridge axis, coupled with the shallow-sill that extends across the entire ocean from Greenland to Europe (the off-axis trace of the hot spot's influence throughout the opening of this ocean basin) provides a natural barrier to deep-water gene-flow between the Mid-Atlantic Ridge and Reykjanes Ridge, to the south and the ridges of the Norwegian-Greenland Sea and Arctic Basin to the north.

[4] Previously, *Cherkashev et al.* [2001] reported geochemical anomalies indicative of geologically recent hydrothermal input in sediment cores from the northern and central Knipovich Ridge. Here we report first evidence for active high-temperature hydrothermal venting along the southern Knipovich ridge, the northernmost component of the Norwegian-Greenland Sea ridge system.

2. Geologic Setting of the Knipovich Ridge

[5] The Knipovich Ridge is located between 73°45′N and 78°35′N to the west of Svalbard and to the east of Greenland in the northernmost Norwegian-Greenland Sea (Figure 1). It extends ~550 km from the Mohns Ridge at its southern limit to the Molloy Deep in the north. Because it is the most northerly section of the Arctic ridge system that lies outside the reach of permanent ice cover, it remains readily accessible to nonspecialist icebreaker research vessels. Present-day plate-motion models indicate an ultra-slow spreading rate of 15–17 mm/yr with a predicted spreading direction at 76°N of 307° [*De Mets et al.*, 1990]. However, the trend of the Knipovich Ridge is oblique to this orientation with a trend that changes from ~002° (000–007°) north of ~75°50′N to ~347° (343–350°) to the south, a

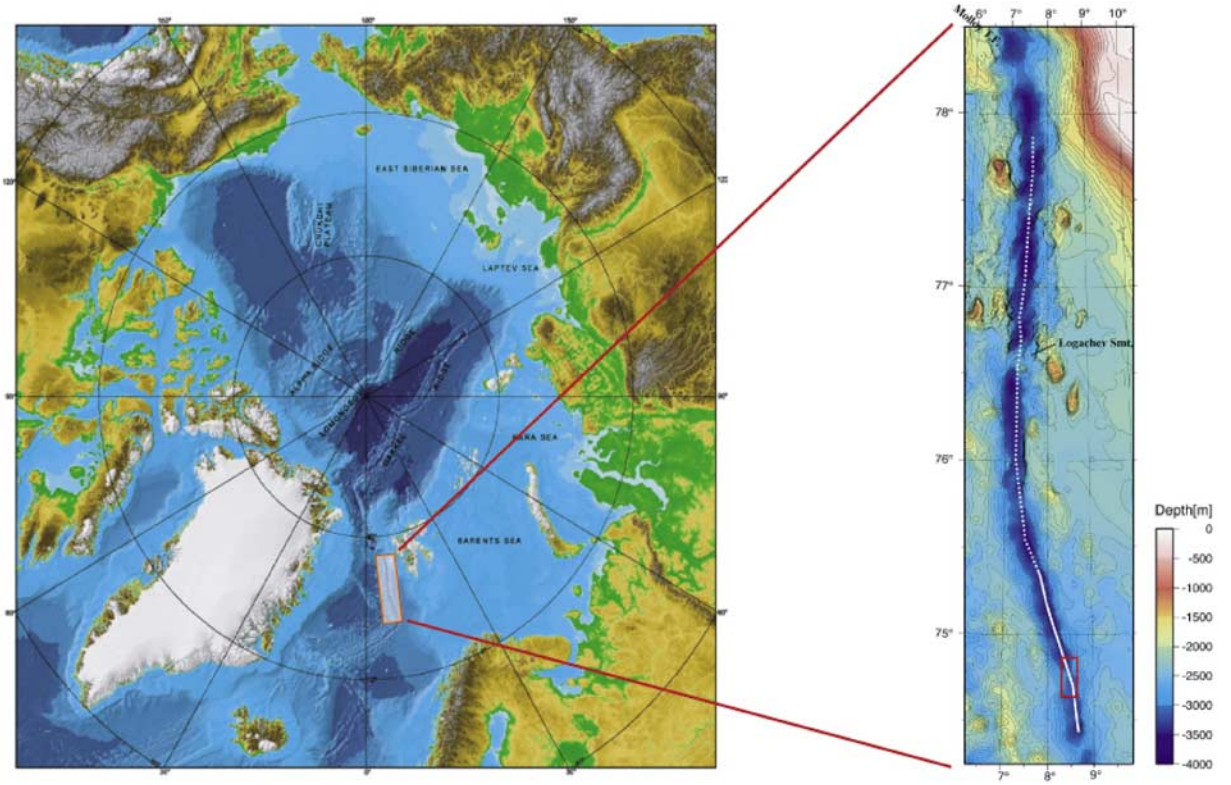

Figure 1. (a) Location of the Knipovich Ridge with (b) detail of the ridge inset. Track line in the box area shows the complete K2000 survey line; boxed area is the area discussed in this paper.

change in obliquity from 35° to 49° from north to south. In recent work, *Okino et al.* [2002] have used along-axis bathymetric profiles and sonar data acquired during the K2K cruise of the R/V *Professor Logachev* [*Tamaki and Cherkashev*, 2000; *Tamaki et al.*, 2001] to investigate the interplay of magmatism and obliquity upon segmentation of this ultra-slow spreading ridge system. That work has demonstrated that second-order segmentation of the Knipovich ridge is dominated by a few large volcanic constructs separated by deep, oblique, nontransform discontinuities, similar to the arrangement already identified on the ultra-slow spreading, oblique SW Indian Ridge [*Mendel et al.*, 1997; *Sauter et al.*, 2001], and as discussed in a paper comparing the ultra-slow SWIR and Arctic (including the Knipovich) ridges by *Dick et al.* [2003].

3. Sampling and Methods

[6] All sampling and data acquisition was conducted aboard the R/V *Professor Logachev* (VNIIO, St. Petersburg, Russia) in September 2000 [*Tamaki and Cherkashev*, 2000; *Tamaki et al.*, 2001]. First, a systematic survey was conducted, combining optical backscatter sensors with deep-tow side-scan investigations, following the methodology first developed by *German et al.* [1996] which used the UK's deep-tow side-scan sonar instrument TOBI. For the current cruise, the deep-tow instrument used was the two-body (depressor weight and sonar "fish") ORETech dual-frequency 30 kHz/100 kHz side-scan sonar navigated in real time using the SIGMA 1001 ("MorFizPribor," Russia) ultra-short baseline (USBL) system installed aboard the R/V *Professor Logachev* [*Tamaki and Cherkashev*, 2000]. During the study reported here, our in situ hydrothermal sensor string (developed at NOC, UK) was deployed above the deep-tow side-scan instrument rather than, as is more typical with the TOBI system, deploying the sensor string beneath the side scan [e.g., *German et al.*, 2000]. At the base of the sensor string, the first of 5 WetLabs LSS-6000 optical backscatter sensors was interfaced to a UMI-2SB15 data-logger (WS Oceans Ltd) equipped with integral CTD sensors and the latter was attached directly to the deep-tow cable, ~25 m above the depressor weight. This depressor, in turn, was separated from the tow-fish by a 110 m

umbilical. After deployment of the tow-fish and depressor, the remainder of the NOC sensor string, comprising four further LSS-6000 sensors each independently connected to the UMI-2SB15 datalogger, were attached at 25 m intervals up the deep-tow cable.

[7] Upon completion of our deep-tow side-scan/sensor-string survey, target sites for further investigation were identified on the basis of optical backscatter signals considered indicative of possible nonbuoyant hydrothermal plumes and hence underlying sources of high-temperature seafloor venting [*Cave and German*, 1998]. These sites were then sampled using a SeaBird 9/11 + CTD-rosette equipped with 10 L Niskin bottles. Water samples obtained from these CTD stations were taken, systematically, throughout the deep-water column, at depths with the highest optical backscatter signals already obtained (there was no optical backscatter sensor available on the R/V *Professor Logachev* CTD system). Water samples were subsequently analyzed, both on board ship and inshore-based laboratories for three key tracers of deep-sea hydrothermal plumes: total dissolvable Mn (TdMn) [*Klinkhammer et al.*, 1986]; dissolved methane (CH_4) [*Charlou et al.*, 1991] and adenosine triphosphate (ATP), a proxy for microbial abundance in the deep ocean [*Karl*, 1980]. Dissolved methane analyses and ATP analyses were conducted shipboard following each CTD cast. By contrast, TdMn analyses were performed post-cruise at the National Oceanography Centre, UK, in a dedicated trace element clean laboratory.

[8] For dissolved methane analyses, samples were drawn into 110 ml glass bottles with a screw-cap lined with a rubber septum, leaving 4 mL of head-space. Bottles were then shaken regularly over several hours to ensure that thorough phase equilibrium between the seawater and head-space was established. Methane concentrations were then determined using head-space analysis of gases extracted by syringe and injected into a portable gas chromatograph equipped with a Flame Ionization Detector (FID). Accuracy in the analysis was 0.05 ppm with seawater methane concentrations determined assuming an initial atmospheric methane concentration of 1.78 ppm [cf. *Bolshakov and Egorov*, 1987].

[9] For TdMn, samples were drawn directly from the CTD-rosette, unfiltered, into acid-cleaned low-density polyethylene 1 L bottles (rinsed three times with sample prior to filling). These samples were then returned to the laboratory and acidified with 1 ml of ultra pure nitric acid for 4 weeks, prior to analysis, to ensure complete dissolution and desorption from bottle walls of all manganese present. The determination of Mn concentrations in these samples was then completed, adhering to an established technique of organic complexation, followed by solvent extraction [*Statham and Burton*, 1986]. Analyses were performed by atomic absorption spectroscopy (AAS) and yielded detection limits of 0.06 nmol/L and an analytical precision of better than 5%.

[10] ATP (adenosine 5′-triphosphate) assays were conducted by measuring bioluminescence on the basis of the luciferin-luciferase reaction [*Egeberg*, 2000]. First, microbial cells were filtered from known volumes of seawater onto 0.2 μm pore size Nuclepore (47 mm diam.) or Isopore (25 mm diam.) filters. These filters were then placed directly into test tubes and microbial ATP extracted and determined using an ATP Bioluminescent Assay Kit (AF-3L1; Toa Electronics Ltd., Japan) and an ATP Tester (AF-70; Toa Electronics Ltd., Japan).

4. Results

4.1. Deep-Tow Hydrothermal Sensor String

[11] During the course of Leg 1 of the K2K Cruise (30 August to 10 September 2000) the ORETech deep-tow side-scan sonar was successfully towed along almost the entire length of the Knipovich Ridge, from 74°30′N to 76°50′N and from 77°19′N to 77°56′N [*Okino et al.*, 2002]. Unfortunately, however, instrumental problems precluded collection of coregistered light-scattering sensor data along all but the southernmost section of the survey, collected over 30 hours, during the first leg of the deep-tow deployment, between 74°30′N and 75°25′N (Figure 1b). All systematic exploration for hydrothermal exploration during the cruise therefore was restricted to the southernmost ~100 km of the ultra-slow spreading Knipovich Ridge. Within the 30 hours taken to conduct this survey, one significant episode of optical backscatter was encountered, detected by 3 of the LSS sensors on the NOC in situ sensor string (sensors 1 and 5 malfunctioned within the first 4 hours of deployment), along a ~2 km section of survey track, extending from 74°46.7′N, 008°28.1′E to 74°47.7′N, 008°27.0′E (Figure 2; red track line in Figure 3a). Maximum anomalies recorded fell in the range 10–15 mV which compares closely with the maximum anomalies reported form the SW

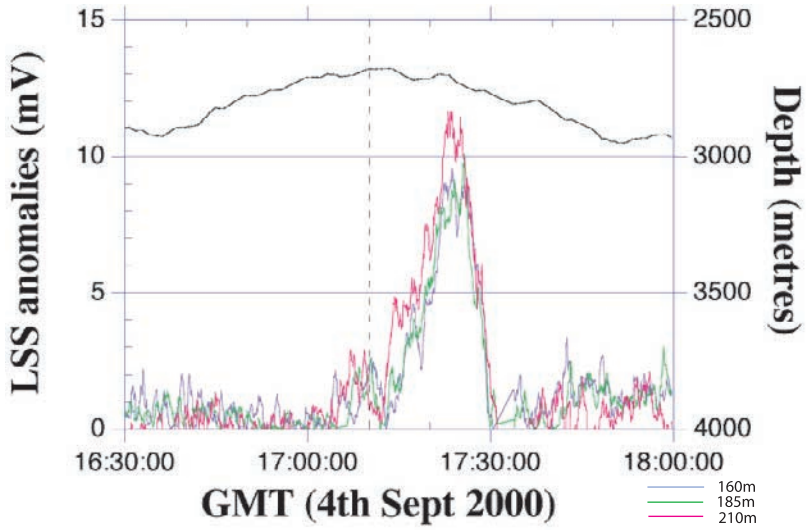

Figure 2. Time, amplitude, and depth of the LSS anomalies of interest, detected from the light-scattering sensor string attached to the deep-tow instrument between 16:30 and 18:00 on 4 September 2000 (74.44°N, 8.66°E to 75.40°N, 7.74°E). Color-coded lines refer to height above the deep-tow instrument.

Indian Ridge, the most directly comparable prior study that we have undertaken, where anomalies were up to 17 mV [*German et al.*, 1998]. These anomalies were recorded at depths of ~2600–2650 m at their upper bound, extending to ~2700–2750 m at their deepest, i.e., 200–350 m shallower than the nearest topographic highs, consistent with what might be predicted for a nonbuoyant hydro-

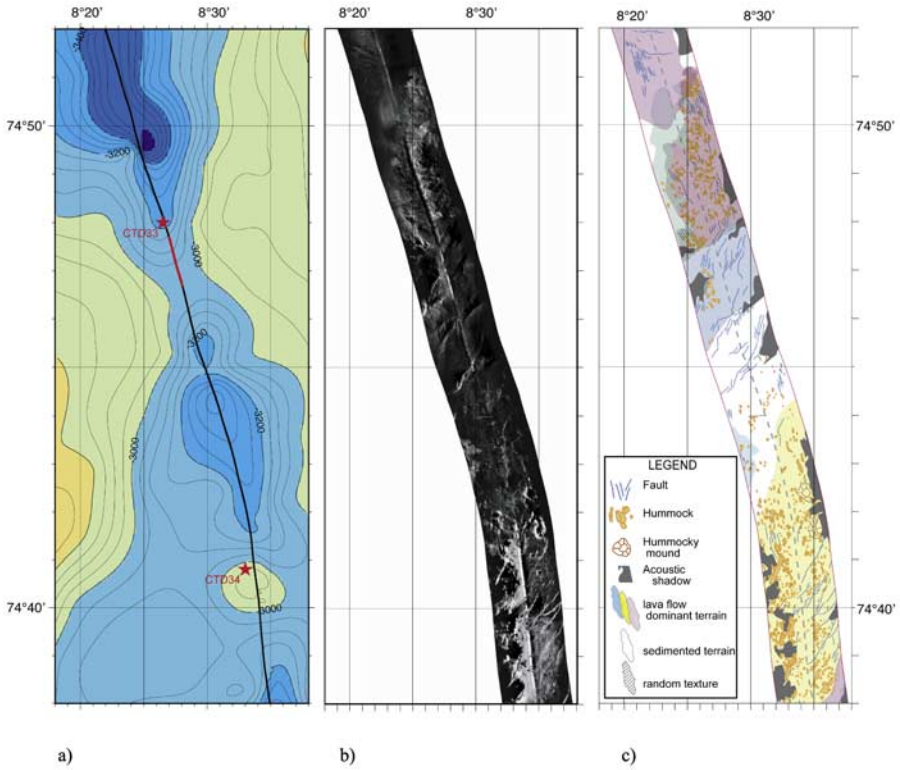

Figure 3. Images of the (a) bathymetry and (b) side-scan data and (c) the interpretation of those data for the study area. In addition, Figure 3a shows CTD stations marked with stars, and the red track line is the area of the LSS survey.

Table 1. Analytical Data for Stations CTD 33 and CTD 34

CTD 33					CTD 34				
Depth, m	Density, kg m^3	TdMn, nM	ATP, pM	CH^4, nM	Depth, m	Density, kg m^3	TdMn, nM	ATP, pM	CH^4, nM
3168	28.0722	1.2	1.65	2.3	2825	28.0718	1.3	1.70	2.0
3000	28.072	1.5	3.13	3.6	2750	28.0721	1.4	0.87	2.2
2900	28.0721	1.5	7.26	3.8	2700	28.0719	1.5	2.68	3.4
2850	28.0722	1.7	10.9	5.6	2650	28.0719	1.5	2.13	3.3
2800	28.072	1.5	1.12	5.3	2600	28.072	1.1	1.22	2.7
2750	28.0719	1.4	1.85	3.5	2550	28.0718	1.0	1.12	2.0
2700	28.0719	1.1	0.50	2.4	2500	28.0717	1.5	1.09	2.2
2650	28.0718	1.4	0.58	3.0	2400	28.0714	1.3	1.06	0.9
2600	28.072	1.3	1.35	2.0	2300	28.0712	1.0	0.89	1.3
2500	28.0716	0.8	0.73	0.5	2280	28.071	1.0	0.63	1.3
2250	28.0707	1.1	1.51	1.3	2100	28.0705	0.8	0.72	1.1
2000	28.0691	0.7	1.70	2.1	2000	28.0697	0.7	0.40	1.0

thermal plume rising from the seafloor in the weakly stratified Norwegian-Greenland Sea.

4.2. CTD Hydrocast Stations

[12] During Leg 2 of the K2K Cruise (10–23 September 2000) two CTD stations were occupied. These were located at either end of the section of deep-tow survey where optical backscatter anomalies were observed to obtain water samples and conduct geochemical analyses that would verify whether these signals were, indeed, hydrothermal in origin (Figure 3a). CTD 33 was occupied at the northern limit of the anomaly at 74°48.0′N, 008°26.5′E (water depth 3185 m); CTD 34 was occupied beyond the southern limit of the anomaly, but directly above a segment-center axial volcanic ridge at 74°40.8′N, 008°33.1′E (water depth 2867 m). At each station, 12-bottle casts were collected throughout the deep water column, targeting depths that coincided with the depth at which the in situ sensor-string anomalies had been detected. Analytical data for samples from both CTD stations are presented in Table 1. Profiles of TdMn, dissolved CH_4 and ATP throughout the deep water column at CTD stations 33 and 34 are presented in Figure 4.

[13] At station CTD 33 a clear maximum in all of TdMn, dissolved CH_4 and ATP is observed at 2850 m water depth with maximum values of 1.7 nM TdMn, 5.6 nM CH_4 and 10.9 pM ATP. This compares with open-ocean background concentrations of 0.2–0.3 nM for total dissolvable Mn (dashed line in Figure 4a) [*Statham and Burton*, 1986], and 0.9 nM for dissolved CH_4 (dashed line in Figure 4b) (A. Egorov, unpublished data, 1999). A second, less pronounced, peak is also apparent in the TdMn and dissolved CH_4 profiles at station CTD 33, at 2650 m depth, but this is not apparent in the ATP profile. Maximum TdMn and CH_4 values in the shallower peak are 1.4 nM and 3.0 nM, respectively, i.e., still significantly above background. At station CTD 34 there is, again, a clear peak in all of the TdMn, dissolved CH_4 and ATP profiles at 2650–2700 m water depth, i.e., 150–200 m shallower that the deep plume at CTD 33. Like the CTD 33 profiles, however, the TdMn and CH_4 profiles at CTD 34 also show a second peak approximately 200 m shallower than the deep plume, in this case at 2500 m water depth (Figure 4). Maximum TdMn, CH_4 and ATP concentrations in the deep plume at CTD 34 are 1.5 nM, 3.4 nM and 2.7 pM. In the shallower (2500 m) peak at CTD 34, TdMn and CH_4 concentrations are 1.5 nM and 2.2 nM. Again, these values are significantly above background.

[14] The chemical anomalies detected in water samples collected from CTDs 33 and 34, during Leg 2 of the K2K research cruise, coincide closely with the depth at which optical backscatter anomalies were detected during Leg 1 of this cruise along the same section of ridge crest (Figure 2).

5. Discussion

5.1. Hydrothermal Plume Anomalies in the Southern Knipovich Ridge Water Column

[15] When high-temperature hydrothermal vents are first emitted from the seabed, they are buoyant and mix turbulently with the overlying seawater. Progressive dilution within the buoyant plume

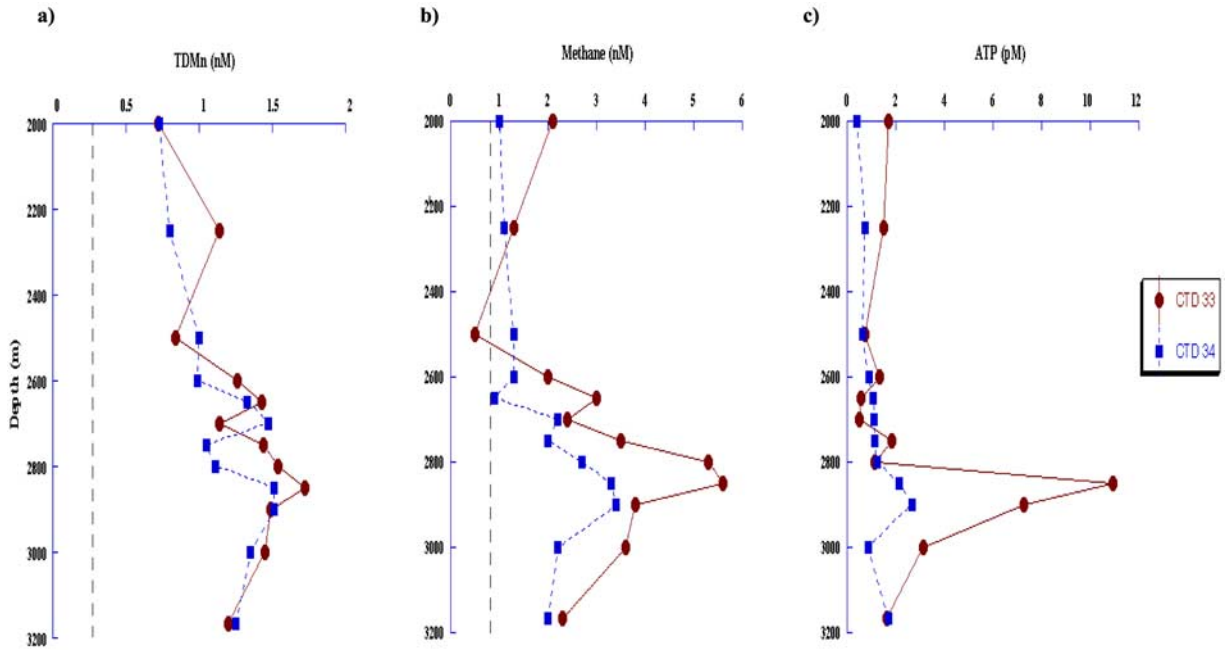

Figure 4. Vertical profiles of (a) TdMn, (b) methane, and (c) ATP concentration versus depth for CTD station 33 and 34. Dotted line indicates background concentrations for TdMn and methane.

proceeds, as the plume rises, until no density contrast persists between the rising plume and the water column into which it intrudes. At this point, the much-diluted plume begins to be dispersed laterally by deep ocean currents [see, e.g., *German and Von Damm*, 2004]. During this emplacement at nonbuoyant plume height, which takes of the order of 1 hour, chemically enriched vent fluids are typically diluted by a factor on the order of 10,000:1 [*Lupton*, 1995]. Because those hydrothermal vent fluids are initially enriched up to 10^6-fold in all of dissolved Fe, Mn and CH_4 when compared to ambient seawater dispersing, nonbuoyant plumes, can continue to carry significant hydrothermal enrichments in dissolved Mn and CH_4 and particulate Fe-oxyhydroxides. It is the latter that give rise to readily detectable in situ optical backscatter signals [*German and Von Damm*, 2004].

[16] The identification that there are significant enrichments of dissolved TdMn, dissolved CH_4 and ATP at a height of a few hundreds of meters above the seabed near 74°N on the Knipovich Ridge, therefore, coincident with water column enrichments in suspended particulate material (as evidenced from optical backscatter), provides compelling evidence that stations CTD 33 and 34 intercepted at least one nonbuoyant hydrothermal plume dispersing away from a source of high-temperature venting. An important further question is: are our data all consistent with a single hydrothermally active vent area or are they indicative of two (or more?) discrete hydrothermal fields? At any given location, the instantaneous height-of-rise of a nonbuoyant plume is a function of the thermal output of the hydrothermal source and the density-stratification of the water column into which it is intruded [e.g., *Speer and Helfrich*, 1995]. In prior work it has been demonstrated that hydrothermal plumes can readily be deflected vertically through 200 m or more as hydrothermal plumes are advected over the rough topography of mid-ocean ridge crests and, further, that the depth of a nonbuoyant hydrothermal plume can vary through 200 m or more over the course of a single tidal cycle [e.g., *Rudnicki and German*, 2002; *German*, 2003].

[17] To examine whether the plume signals measured at stations CTD 33 and 34 are sourced from different hydrothermal fields or might, instead, derive from a common seafloor source, their TdMn, CH_4 and ATP concentration profiles are replotted in Figure 5 against density rather than depth. What is immediately apparent from all three tracers' profiles is that the deep maximum for all of TdMn, CH_4 and ATP at both stations occupies exactly the same density surface ~28.072 kg m^3. What is also apparent from these three profiles is that the maximum chemical anomalies seen at this

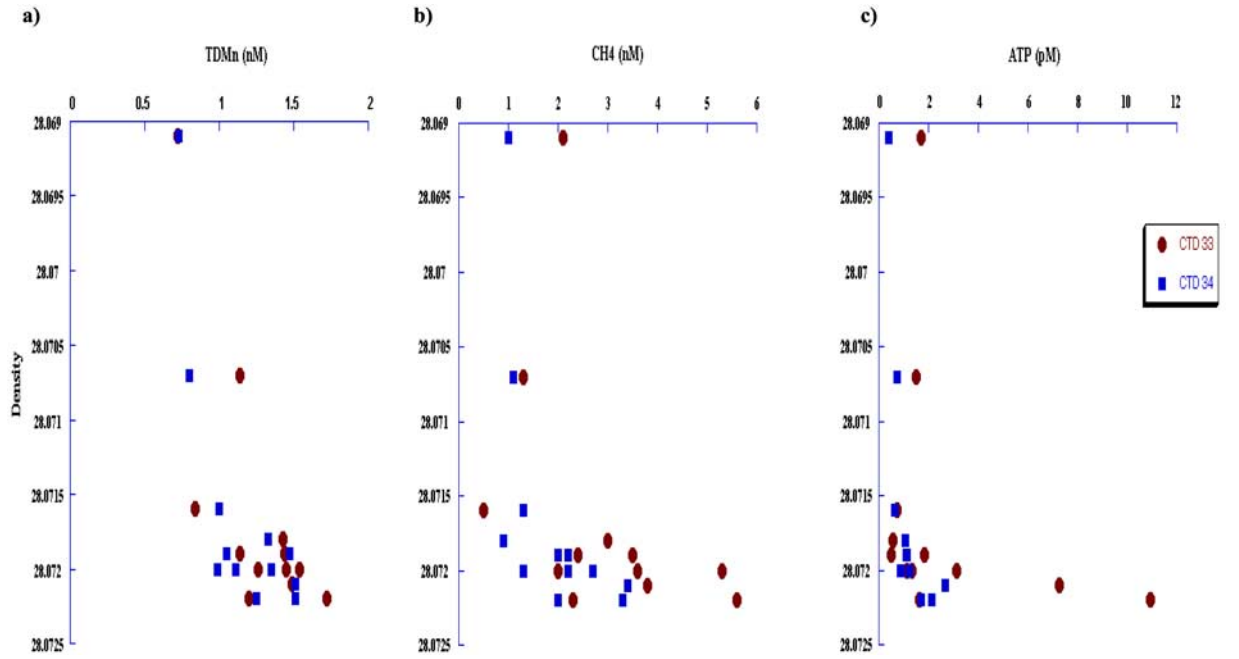

Figure 5. Distribution of (a) TdMn, (b) methane, and (c) ATP for CTD station 33 and 34 plotted against density.

density horizon are greater at CTD station 33 than they are at station CTD 34. The differences are rather subtle for TdMn between the two stations, set ~12 km apart, but the respective profiles for dissolved methane differ by a factor of ~2, and by a factor of 4 for ATP. In the case of ATP, using a known concentration of 4 mg bacterial ATP for 1g bacterial carbon [*Karl*, 1980] and an approximation that 1g bacterial carbon equates to 10^{14} bacterial cells [*Gerlach*, 1978] we can estimate that the difference between plume values at stations CTD 33 and CTD 34 equates to a reduction from 160 × 10^6 to 40 × 10^6 cells/liter. These data are all consistent with a common nonbuoyant hydrothermal plume that is dispersing from north to south along-axis, away from a source near station CTD 33, toward CTD 34. The degree of change between adjacent stations in terms of the three different tracers investigated (TdMn, CH_4, and ATP) is also consistent with what is known about the relative reactivities of different tracers released into nonbuoyant hydrothermal plumes. Oxidation of dissolved Mn proceeds rather slowly, and once oxidized and precipitated, fine-grained Mn-rich particulates may remain suspended over long distances through the water column exhibiting quasi-conservative water column behavior [*Klinkhammer et al.*, 1986]. By contrast, dissolved methane is much more unstable in the water column and shows much greater reactivity/nonconservative behavior [e.g., *Kadko et al.*, 1990]. Finally, ATP concentrations decrease by ~75% between stations 33 and 34. Although microbial data from nonbuoyant hydrothermal plumes remain sparse [*Cowen and Li*, 1991; *Sunamura et al.*, 2004], these data do not appear unreasonable: ATP concentrations may be reduced as a result of cellular conversion to ADP, or degraded when cells die.

5.2. Geologic Setting of Southern Knipovich Ridge Hydrothermal Vents

[18] Station CTD 34, located to the south of the maximum plume anomalies, was occupied directly above a topographic high which has been unambiguously identified, from coregistered side-scan sonar data, to represent one of the pronounced axial volcanic highs that define second-order ridge-segment centers along the ultra-slow spreading Knipovich Ridge [*Okino et al.*, 2002]. The side-scan backscatter from this particular seamount, indeed, is the strongest observed anywhere along the southern Knipovich Ridge survey. By contrast, the higher strength hydrothermal anomalies identified by both the LSS sensor string (Figure 3) and from chemical analyses of CTD 33 samples (Figures 4 and 5) are coincident with an along-axis topographic low, lying in between adjacent, en echelon segment centers [cf. *Parson et al.*, 1993]. Rather than simply indicating flat, sedi-

mented terrain at this location, however, the coregistered side-scan sonar data immediately underlying this section of the ridge axis are rather enigmatic (M. Asada, manuscript in preparation, 2007). The backscattering strength is higher than flat sedimented terrain, but the seafloor texture is rough and quite dissimilar to what would be expected from smooth or hummocky lava-flows. Further, many short lineaments (faults, fissures or other unknown linear features) can be seen, with azimuths that are randomly distributed (Figure 3c). These features therefore can best be categorized as ''random high side-scan backscatter data''; however, they also bear a marked resemblance to TOBI side-scan sonar data from portions of the SW Indian Ridge (a comparably ultra-slow spreading section of ridge crest) that are dominated by serpentinization of ultramafic lithologies outcropping at the seafloor [*Sauter et al.*, 2001].

[19] Two different kinds of ultramafic-influenced hydrothermal systems have been found in the north Atlantic previously. At Lost City [*Kelley et al.*, 2005] and Saldanha [*Dias and Barriga*, 2006] low-temperature venting is observed fuelled, possibly, by exothermic serpentinization reactions alone. Such systems, however, do not generate the particle-laden, metal-rich plumes reported here. More relevant to this work data are the Rainbow [*German et al.*, 1996] and Logachev [*Cherkashev et al.*, 2000] fields that exhibit high-temperature venting reminiscent of conventional black smoker fields but which are hosted in highly tectonized terrain and, chemical signatures reveal, are at least partially influenced by chemical reactions with ultramafic, as well as gabbroic rocks. In 3 of the 6 sites located on the eastern SWIR by *German et al.* [1998] and at least 6 out of 14 hydrothermally active stations identified farther West on the Oblique Super-Segment (OSS) of the SWIR [*Bach et al.*, 2002] water column plume signals indicative of *high-temperature* seafloor venting were attributed to being hosted in ultramafic rock-types and/or under tectonic rather than volcanic controls similar to Rainbow and Logachev. Along the Gakkel Ridge, by contrast, *Edmonds et al.* [2003] concluded that no more than perhaps one (at most) of 12 sites they identified were colocated with anything other than axial volcanic centers comparable in size and nature to that observed near CTD 34 (Figure 2).

[20] In prior work *Charlou et al.* [1991] reported extremely high CH_4 to TdMn ratios (>25:1) for samples collected at 15°N on the Mid-Atlantic Ridge which they interpreted must result from serpentinization of exposed ultramafic rocks at this site. Subsequently analyses of hydrothermal plume samples overlying the Rainbow high-temperature ultramafic-influenced vent site on the MAR revealed methane to TdMn ratios of approximately 1:1 [*Jean-Baptiste et al.*, 2004]. Although this ratio is significantly lower than that for the data from 15°N, it is, nevertheless, significantly higher than values obtained from volcanically hosted Atlantic hydrothermal plumes: TAG = 0.4 [*Charlou et al.*, 1991]; Steinaholl = 0.3 [*German et al.*, 1994]. Data from station CTD 33 and 34 in this study show methane to manganese ratio at plume height of 2-3:1, i.e., most directly comparable to the Rainbow hydrothermal plume data of *Jean-Baptiste et al.* [2004]. This provides a further, independent, line of evidence that the plume signals reported here result from a high-temperature hydrothermal source hosted, at least partially, in ultramafic rocks.

[21] On the adjacent Gakkel Ridge (where ridge alignment is orthogonal to spreading direction and second-order segmentation is largely absent) evidence for hydrothermal venting is almost exclusively associated with neovolcanic activity [*Edmonds et al.*, 2003; *Baker et al.*, 2004]. By contrast, orientation of the southern Knipovich Ridge is highly oblique [*Okino et al.*, 2002], as is considered to be the general case for ultra-slow spreading ridges [*Dick et al.*, 2003] and, here, clear evidence for ultramafic hosted, tectonically controlled high-temperature venting has been revealed. Such sites are of particular interest to those interested in studying processes such as abiotic organic synthesis, pre-biotic chemistry and the origins of life [e.g., *Shock*, 1996; *Holm and Charlou*, 2001]. Our findings from the Arctic ultra-slow ridge system, coupled with comparable data from the SW Indian Ridge, as well as initial findings on the Mid-Atlantic Ridge support hypotheses [e.g., *German*, 2004] that such systems may be widespread along all the Earth's slow and ultra-slow spreading ridges.

6. Summary

[22] 1. We have identified first evidence for high-temperature hydrothermal venting on the Southern Knipovich Ridge.

[23] 2. Plume signals were first detected using in situ optical backscatter sensors suspended from a deep-tow side-scan sonar instrument as it was towed along the ridge axis and subsequently confirmed by analyzing targeted CTD-rosette samples for diagnostic tracers of plume activity: TdMn, dissolved CH_4 and ATP (a proxy for microbial activity).

[24] 3. Data from two CTD stations are consistent with a common hydrothermal plume dispersing along an isopycnal surface. From concentration gradients between the two stations, we infer a direction of flow, from north to south, toward an axial volcanic ridge. This implies that the source of the anomalies observed is NOT associated with a nearby volcanic center of the kind that defines second-order segmentation on the Knipovich Ridge.

[25] 4. Instead, the hydrothermal source we have identified appears to be hosted in tectonically dominated terrain reminiscent of serpentenizing ultramafic outcrops. High-temperature venting within ultramafic rocks has only been reported to occur, previously, at the Rainbow and Logachev hydrothermal fields on the slow-spreading MAR although similar interpretations of plume data have also been proposed for the ultra-slow SWIR.

[26] 5. Plume height methane to manganese ratios on the southern Knipovich Ridge (2–3:1) are higher than volcanically hosted Atlantic plumes and more comparable to values from the Rainbow hydrothermal plume. This provides further compelling evidence that the source of the plume anomalies we have identified should be a high-temperature hydrothermal field hosted, at least partially, in serpentenizing ultramafic rocks.

Acknowledgments

[27] The authors would like to thank the team of the R/V *Professor Logachev* for conducting onboard investigations. Thanks also go to Kathy Crane, who initiated and organized the expedition. The ''Knipovich-2000'' cruise was financed by the Ministry of Education, Culture and Sport of Japan. Connelly and German were funded by NERC grant NER/B/S/2000/00755, NERC Core Strategic Funding at NOC, and the ChEss project of the Census of Marine Life. The authors wish to thank two reviewers who provided valuable input to the paper.

References

Bach, W., N. R. Banerjee, H. J. B. Dick, and E. T. Baker (2002), Discovery of ancient and active hydrothermal systems along the ultra-slow spreading Southwest Indian Ridge 10°–16°E, *Geochem. Geophys. Geosyst.*, *3*(7), 1044, doi:10.1029/2001GC000279.

Baker, E. T., and C. R. German (2004), On the global distribution of mid-ocean ridge hydrothermal vent fields, in *The Thermal Structure of the Oceanic Crust and the Dynamics of Seafloor Hydrothermal Circulation*, *Geophys. Monogr. Ser.*, vol. 148, pp. 245–266, AGU, Washington, D. C.

Baker, E. T., H. N. Edmonds, P. J. Michael, W. Bach, H. J. B. Dick, J. E. Snow, S. L. Walker, N. R. Banerjee, and C. H. Langmuir (2004), Hydrothermal venting in magma deserts: The ultraslow-spreading Gakkel and Southwest Indian Ridges, *Geochem. Geophys. Geosyst.*, *5*, Q08002, doi:10.1029/2004GC000712.

Bolshakov, A. M., and A. V. Egorov (1987), On the application of phase-equilibrium degassing method for gasomatric investigation, *Okeanologiya*, *27*, 861–862.

Cave, R. R., and C. R. German (1998), Hydrothermal plume detection in the deep ocean-A combination of technologies, *Underwater Technol.*, *23*, 71–75.

Charlou, J.-L., H. Bougault, P. Appriou, T. Nelsen, and P. Rona (1991), Different TDM/CH4 hydrothermal plume signatures: TAG site at 26°N and serpentinized ultrabasic diapir at 15°05′N on the Mid-Atlantic Ridge, *Geochim. Cosmochim. Acta*, *55*(11), 3209–3222.

Cherkashev, G. A., A. M. Ashadze, and A. V. Gebruk (2000), New fields with manifestations of hydrothermal activity in the Logatchev area (14°N, Mid-Atlantic Ridge), *InterRidge News*, *9*, 26–27.

Cherkashev, G. A., et al. (2001), The Knipovich Ridge Rift Zone: Evidence from the Knipovich 2000 Expedition, *Dokl. Acad. Sci. USSR, Earth Sci. Ser., Engl. Transl.*, *378*(4), 420–423.

Corliss, J. B., et al. (1979), Submarine thermal springs on the Galapagos Rift, *Science*, *203*, 1073–1083.

Cowen, J. P., and Y. H. Li (1991), The influence of a changing bacterial community on trace-metal scavenging in a deep-sea particle plume, *J. Mar. Res.*, *49*, 517–542.

De Mets, C., R. G. Gordon, D. F. Argus, and S. Stein (1990), Current plate motions, *Geophys. J. Int.*, *101*, 425–478.

Dias, A. S., and F. J. A. S. Barriga (2006), Mineralogy and geochemistry of hydrothermal sediments from the serpentinite-hosted Saldanha hydrothermal field (36°34′N: 33°26′W) at MAR, *Mar. Geol.*, *225*, 157–175.

Dick, H. J. B., J. Lin, and H. Schouten (2003), An ultraslow-spreading class of ocean ridge, *Nature*, *426*, 405–412.

Edmonds, H. N., P. J. Michaels, E. T. Baker, D. P. Connelly, J. E. Snow, C. H. Langmuir, H. J. B. Dick, C. R. German, and D. W. Graham (2003), Discovery of abundant hydrothermal venting on the ultraslow-spreading Gakkel ridge in the Arctic Ocean, *Nature*, *421*, 252–256.

Egeberg, P. K. (2000), Adenosine 5′-triphosphate (ATP) as a proxy for bacteria numbers in deep-sea sediments and correlation with geochemical parameters (Site 994), *Proc. Ocean Drill. Program Sci. Results*, *164*, 393–398.

Gerlach, S. A. (1978), Food-chain relationships in subtidal and silty sand marine sediments and the role of meiofauna in stimulating bacterial productivity, *Oecologia*, *3*, 55–70.

German, C. R. (2003), Hydrothermal activity on the eastern SWIR (50°–70°E): Evidence from core-top geochemistry, 1887 and 1998, *Geochem. Geophys. Geosyst.*, *4*(7), 9103, doi:10.1029/2003GC000522.

German, C. R. (2004), Hydrothermal exploration and astrobiology: Oases for life in distant oceans?, *Int. J. Astrobiol.*, *3*, 81–95.

German, C. R., and Von K. L. Damm (2004), Hydrothermal processes, in *Treatise on Geochemistry*, vol. 6, *The Oceans*

and Marine Geochemistry, edited by K. K. Turekian and H. D. Holland, pp. 181–222, Elsevier, Oxford, UK.

German, C. R., et al. (1994), Hydrothermal activity on the Reykjanes Ridge: The Steinaholl vent field at 65°06′N, *Earth Planet. Sci. Lett.*, *121*(3–4), 647–654.

German, C. R., L. M. Parson, and HEAT Scientific Team (1996), Hydrothermal exploration near the Azores Triple Junction: Tectonic control of venting at slow spreading ridges, *Earth Planet. Sci. Lett.*, *138*, 93–104.

German, C. R., E. T. Baker, C. Mevel, K. Tamaki, and FUJI Science Team (1998), Hydrothermal activity along the southwest Indian ridge, *Nature*, *395*, 490–493.

German, C. R., R. A. Livermore, E. T. Baker, N. I. Bruguier, D. P. Connelly, A. P. Cunningham, P. Morris, I. P. Rouse, P. J. Statham, and P. A. Tyler (2000), Hydrothermal plumes above the East Scotia Ridge: An isolated high-latitude back-arc spreading centre, *Earth Planet. Sci. Lett.*, *184*, 241–250.

Holm, N., and J.-L. Charlou (2001), Initial indications of abiotic formation of hydrocarbons in the Rainbow ultramafic hydrothermal system, Mid-Atlantic Ridge, *Earth Plant. Sci. Lett.*, *191*, 1–8.

Jean-Baptiste, P., E. Fourré, J. L. Charlou, C. German, and J. Radford-Knoery (2004), Helium isotopes at the Rainbow hydrothermal site (Mid-Atlantic Ridge, 36°14′N), *Earth Planet. Sci. Lett.*, *221*, 325–335.

Kadko, D. C., N. D. Rosenberg, J. E. Lupton, R. W. Collier, and M. D. Lilley (1990), Chemical reaction rates and entrainment within the Endeavour Ridge hydrothermal plume, *Earth Planet. Sci. Lett.*, *99*, 315–335.

Karl, D. M. (1980), Cellular nucleotide measurements and applications in microbial ecology, *Microbiol. Rev.*, *44*, 739–746.

Kelley, D. S., et al. (2005), A serpentinite-hosted ecosystem: The lost city hydrothermal field, *Science*, *307*, 1428–1434.

Klinkhammer, G., H. Elderfield, M. J. Greaves, P. Rona, and T. A. Nelsen (1986), Manganese geochemistry near high-temperature vents in the Mid-Atlantic Ridge rift valley, *Earth Planet. Sci. Lett.*, *80*, 230–240.

Lupton, J. E. (1995), Hydrothermal plumes: Near and far field, in *Seafloor Hydrothermal Systems: Physical, Chemical, Biological, and Geological Interactions*, *Geophys. Monogr. Ser.*, vol. 91, edited by S. E. Humphris et al., pp. 317–346, AGU, Washington, D. C.

Mendel, V., D. Sauter, L. Parson, and J. R. Vanney (1997), Segmentation and morphometric variations along a super slow-spreading center: The Southwest Indian Ridge (57°E–70°E), *Mar. Geophys. Res.*, *19*, 505–533.

Okino, K., D. Curewitz, M. Asada, K. Tamaki, P. Vogt, and K. Crane (2002), Preliminary analysis of the Knipovich Ridge segmentation: Influence of focused magmatism and ridge obliquity on an ultraslow spreading system, *Earth Planet. Sci. Lett.*, *202*, 275–288.

Parson, L. M., et al. (1993), En echelon axial volcanic ridges at the Reykjanes ridge: A life cycle of volcanism and tectonics, *Earth Planet. Sci. Lett.*, *117*, 73–87.

Rudnicki, M. D., and C. R. German (2002), Temporal variability of the hydrothermal plume above the Kairei vent field, 25°S, Central Indian Ridge, *Geochem. Geophys. Geosyst.*, *3*(2), 1010, doi:10.1029/2001GC000240.

Sauter, D., P. Patriat, C. Rommevaux-Jestin, M. Cannat, and A. Briais (2001), The Southwest Indian Ridge between 49°15′E and 57°E: Focused accretion and magma redistribution, *Earth Planet. Sci. Lett.*, *192*, 303–317.

Shock, E. L. (1996), Hydrothermal systems as environments for the emergence of life, in *Evolution of Hydrothermal Ecosystems on Earth (and Mars?)*, *Ciba Foundation Symp. Ser.*, vol. 202, pp. 40–60, John Wiley, Chichester, U. K.

Speer, K. G., and K. R. Helfrich (1995), Hydrothermal plumes: A review of flow and fluxes, in *Hydrothermal Vents and Processes*, edited by L. M. Parson, C. L. Walker, and D. R. Dixon, *Geol. Soc. Spec. Publ.*, *87*, 373–385.

Statham, P. J., and J. D. Burton (1986), Dissolved manganese in the North Atlantic Ocean, 0–35°N, *Earth Planet. Sci. Lett.*, *79*, 55–65.

Sunamura, M., Y. Higashi, C. Miyako, J. Ishibashi, and A. Maruyama (2004), Two bacteria phylotypes are predominant in the Suiyo seamount hydrothermal plume, *Appl. Environ. Microbiol.*, *70*, 1190–1198.

Tamaki, K., and G. Cherkashev (2000), Knipovich-2000 onboard cruise report, Ocean Res. Inst., Univ. of Tokyo, Tokyo.

Tamaki, K., G. Cherkashev, and K2K Team (2001), Japan-Russia cooperation at the Knipovich Ridge in the Arctic Sea, *InterRidge News*, *10*(1), 48–52.

Tyler, P. A., C. R. German, E. Ramirez-Llodra, and C. L. Van Dover (2002), ChEss: Understanding the biogeography of chemosynthetic ecosystems*Oceanol. Acta*, *25*, 227–241.

Van Dover, C. L., C. R. German, K. G. Speer, L. M. Parson, and R. C. Vrijenhoek (2002), Marine biology: Evolution and biogeography of deep-sea vent and seep invertebrates, *Science*, *295*, 1253–1257.